J|A|C|S ARTICLES

Co-adsorption and Separation of CO_2-CH_4 Mixtures in the Highly Flexible MIL-53(Cr) MOF

Lomig Hamon,[†] Philip L. Llewellyn,[‡,*] Thomas Devic,[§] Aziz Ghoufi,[ǁ] Guillaume Clet,[⊥] Vincent Guillerm,[§] Gerhard D. Pirngruber,[†,*] Guillaume Maurin,[ǁ] Christian Serre,[§] Gordon Driver,[‡] Wouter van Beek,[#,∇] Elsa Jolimaître,[†] Alexandre Vimont,[⊥] Marco Daturi,[⊥] and Gérard Férey[§]

IFP, Direction Catalyse et Séparation, rond-point de l'échangeur de Solaize, 69360 Solaize, France, Laboratoire Chimie Provence, UMR CNRS 6264-Universités d'Aix-Marseille I, II, & III, Centre de Saint Jérôme, 13397 Marseille cedex 20, France, Institut Lavoisier, UMR CNRS 8180-Université de Versailles St Quentin en Yvelines, 45 avenue des Etats-Unis, 78035 Versailles, France, Institut Charles Gerhardt, UMR 5253 CNRS-UM2-ENSCM, Université de Montpellier II, Place E. Bataillon, 34095 Montpellier cedex 05, France, Laboratoire Catalyse et Spectrochimie, ENSICAEN, Université de Caen Basse Normandie, CNRS, boulevard du Maréchal Juin, 14050 Caen, France, SNBL at ESRF, rue Jules Horowitz, 38043 Grenoble, France, and Dipartimento di Scienze e Tecnologie Avanzate, Università del Piemonte Orientale "A. Avogadro", 15121 Alessandria, Italy

Received September 15, 2009; E-mail: philip.llewellyn@univ-provence.fr; gerhard.pirngruber@ifp.fr

Abstract: The present study attempts to understand the use of the flexible porous chromium terephthalate $Cr(OH)(O_2C-C_6H_4-CO_2)$ denoted MIL-53(Cr) (MIL = Material from Institut Lavoisier) for the separation of mixtures of CO_2 and CH_4 at ambient temperature. The coadsorption of CO_2 and CH_4 was studied by a variety of different techniques. In situ synchrotron X-ray Powder Diffraction allowed study of the breathing of the solid upon adsorption of the gas mixtures and simultaneously measured Raman spectra yielded an estimation of the adsorbed quantities of CO_2 and CH_4, as well as a quantification of the fraction of the narrow pore (NP) and the large pore (LP) form of MIL-53. Quantitative coadsorption data were then measured by gravimetry and by breakthrough curves. In addition, computer simulation was performed to calculate the composition of the adsorbed phase in comparison with experimental equilibrium isotherms and breakthrough results. The body of results shows that the coadsorption of CO_2 and CH_4 leads to a similar breathing of MIL-53(Cr) as with pure CO_2. The breathing is mainly controlled by the partial pressure of CO_2, but increasing the CH_4 content progressively decreases the transformation of LP to NP. CH_4 seems to be excluded from the NP form, which is filled exclusively by CO_2 molecules. The consequences in terms of CO_2/CH_4 selectivity and the possible use of MIL-53(Cr) in a PSA process are discussed.

Introduction

Metal organic framework materials (MOFs) are an interesting class of porous solids with high potential for hydrogen[1−4] storage, carbon dioxide[5−10] capture, gas separation and purification,[11−13] liquid separation,[14−17] catalysis,[11] and drug delivery.[18,19] MOFs are synthesized from polytopic organic ligands and metal oxide clusters giving rise to crystalline

---

[†] IFP, Direction Catalyse et Séparation.
[‡] Laboratoire Chimie Provence, UMR CNRS 6264-Universités d'Aix-Marseille I, II & III.
[§] Institut Lavoisier, UMR CNRS 8180-Université de Versailles St Quentin en Yvelines.
[ǁ] Institut Charles Gerhardt, UMR 5253 CNRS-UM2-ENSCM, Université de Montpellier II.
[⊥] Laboratoire Catalyse et Spectrochimie, ENSICAEN, Université de Caen Basse Normandie.
[#] SNBL at ESRF.
[∇] Dipartimento di Scienze e Tecnologie Avanzate, Università del Piemonte Orientale "A. Avogadro".

(1) Latroche, M.; Surble, S.; Serre, C.; Mellot-Draznieks, C.; Llewellyn, P. L.; Lee, J. H.; Chang, J. S.; Jhung, S. H.; Ferey, G. *Angew. Chem., Int. Ed.* **2006**, *45* (48), 8227–8231.
(2) Liu, Y. L.; Eubank, J. F.; Cairns, A. J.; Eckert, J.; Kravtsov, V. C.; Luebke, R.; Eddaoudi, M. *Angew. Chem., Int. Ed.* **2007**, *46* (18), 3278–3283.
(3) Li, Y.; Yang, R. T. *Langmuir* **2007**, *23* (26), 12937–12944.
(4) Rosi, N. L.; Eckert, J.; Eddaoudi, M.; Vodak, D. T.; Kim, J.; O'Keeffe, M.; Yaghi, O. M. *Science* **2003**, *300* (5622), 1127–1129.

(5) Bourrelly, S.; Llewellyn, P. L.; Serre, C.; Millange, F.; Loiseau, T.; Ferey, G. *J. Am. Chem. Soc.* **2005**, *127* (39), 13519–13521.
(6) Furukawa, H.; Miller, M. A.; Yaghi, O. M. *J. Mater. Chem.* **2007**, *17* (30), 3197–3204.
(7) Llewellyn, P. L.; Bourrelly, S.; Serre, C.; Vimont, A.; Daturi, M.; Hamon, L.; De Weireld, G.; Chang, J. S.; Hong, D. Y.; Hwang, Y. K.; Jhung, S. H.; Ferey, G. *Langmuir* **2008**, *24* (14), 7245–7250.
(8) Llewellyn, P. L.; Bourrelly, S.; Serre, C.; Filinchuk, Y.; Ferey, G. *Angew. Chem., Int. Ed.* **2006**, *45* (46), 7751–7754.
(9) Serre, C.; Bourrelly, S.; Vimont, A.; Ramsahye, N. A.; Maurin, G.; Llewellyn, P. L.; Daturi, M.; Filinchuk, Y.; Leynaud, O.; Barnes, P.; Ferey, G. *Adv. Mater.* **2007**, *19* (17), 2246–2251.
(10) Millward, A. R.; Yaghi, O. M. *J. Am. Chem. Soc.* **2005**, *127* (51), 17998–17999.
(11) Mueller, U.; Schubert, M.; Teich, F.; Puetter, H.; Schierle-Arndt, K.; Pastre, J. *J. Mater. Chem.* **2006**, *16* (7), 626–636.
(12) Wang, Q. M.; Shen, D. M.; Bulow, M.; Lau, M. L.; Deng, S. G.; Fitch, F. R.; Lemcoff, N. O.; Semanscin, J. *Microporous Mesoporous Mater.* **2002**, *55* (2), 217–230.
(13) Hamon, L.; Serre, C.; Devic, T.; Loiseau, T.; Millange, F.; Ferey, G.; De Weireld, G. *J. Am. Chem. Soc.* **2009**, *131* (25), 8775–8777.

materials.[20,21] Their pore size and shape can be easily tuned by changing either organic ligands or metallic clusters. The structures of MOFs are typically rigid but some of them exhibit an extraordinary structure flexibility upon adsorption/desorption of specific gases or liquids.[5,7,22−25] One of the most spectacular examples is the series of metal terephthalates MIL-53 or $M(OH)(O_2C-C_6H_4-CO_2)$,[26] $M = Al^{3+}$, Cr^{3+} or Fe^{3+},[26] which are able to adjust their pore size and shape in response to the adsorption of polar molecules (CO_2, H_2O) and linear hydrocarbons, except methane.[9,13,26−28] Starting from the so-called *large-pore* form (LP) with almost rectangular pores (0.85 × 0.85 nm), the structure switches to the so-called *narrow-pore* (NP) form, with trapezoidal pores (0.26 × 1.36 nm) upon adsorption of the above-mentioned gases or vapors. Depending on the adsorbed species, the unit cell volume of the NP form may be 40% lower than that of the LP version. As the adsorbate loading increases, the structure switches back from the NP to the LP forms. In contrast, MIL-53(Cr) does not undergo any structural modifications upon adsorption of light hydrocarbons (CH_4) and other small, nonpolar molecules including Ar, He, N_2, and O_2.[8,29,30]

The occurrence of breathing upon adsorption depends on the difference in free energy between the LP and NP host structure (ΔF_{host}), as well as on the pore volumes and the adsorption affinities of the two structural forms.[28] For the LP−NP transition to occur, the positive ΔF_{host} (under vacuum, the LP structure is the most stable form at room temperature) must be compensated by a significantly stronger adsorption affinity in the NP form. This is the case, for example, for CO_2, but not for CH_4. At higher loadings, the structure with the larger pore volume is always favored. Hence, an NP−LP transition occurs above a certain "gate-opening" pressure. This theoretical thermodynamic concept is in qualitative agreement with the experimental observations.[30] During the gradual transition from NP to LP above the gate-opening pressure, the MIL-53(Cr) solid does not adopt any intermediate structure (with an intermediate unit cell volume), but consists of a mixture of the NP and LP forms, the proportion of the latter gradually increasing with pressure. This statement is based on evidence from both simulations,[31] XRD and in situ IR spectroscopy.[9]

While the role of adsorption of single components on the flexibility is now quite well established, knowledge is still scarce about the breathing behavior in the presence of gas mixtures, in particular for those containing a component that provokes breathing and another one that does not. The adsorption of $CO_2−CH_4$ mixtures on MIL-53(Cr) falls into this latter category; studying this system is therefore of high fundamental interest.

At the same time, the separation of CO_2 and CH_4 is also very relevant for industrial applications. The separation of $CO_2−CH_4$ is typically done using solvents (amines or K_2CO_3 in aqueous solution) that remove CO_2 from the gas mixture. These basic solvents are very selective toward CO_2, but their regeneration by heating consumes a large amount of energy. Pressure Swing Adsorption processes (PSA) are energetically more efficient and reliable, but adsorbents with a high selectivity for CO_2 and a high working capacity are still needed. A general shortcoming of adsorption-based CO_2 separation processes is also that contaminants like H_2O and H_2S usually need to be removed upstream of the PSA because they would otherwise be preferentially adsorbed in the bed and reduce its capacity for CO_2. Recent studies indicated that MIL-53(Al) is a promising adsorbent for $CO_2−CH_4$ separations.[32,33] In addition to a high CO_2 adsorption capacity and a good stability in the presence of contaminants (H_2O, H_2S),[13,34] it shows a good $CO_2−CH_4$ selectivity, ranging from 8 to 4.[32] Functionalization with amino groups further improves the selectivity, which might be partially due to changes in the breathing behavior.[33] Both above-cited works show the separation potential of MIL-53, but the role of the structure flexibility in the separation was only very briefly mentioned and certainly not fully understood. Moreover, the adsorption/desorption of pure CO_2 on MIL-53 follows a hysteresis,[8,9] which will have a large impact on the performance within a cyclic adsorption−desorption process like PSA. To date, the impact of the coadsorption of CH_4 on the hysteresis remains unknown.

In order to address these important issues, this work reports an in-depth study of the breathing of MIL-53(Cr) upon adsorption of three different $CO_2−CH_4$ binary mixtures, by in situ XRPD coupled with Raman spectroscopy, gravimetric coadsorption measurements, and breakthrough curves. This experimental investigation is completed by a modeling approach able to capture the coadsorption mechanism at the microscopic scale. The objective is 2-fold: (i) explaining in detail the effect of the coadsorption on the breathing of the MIL-53 solid and comparing the separation selectivity of its *large pore* (LP) and *narrow pore* (NP) forms; (ii) evaluating the potential of MIL-

(14) Alaerts, L.; Kirschhock, C. E. A.; Maes, M.; van der Veen, M. A.; Finsy, V.; Depla, A.; Martens, J. A.; Baron, G. V.; Jacobs, P. A.; Denayer, J. E. M.; De Vos, D. E. *Angew. Chem., Int. Ed.* **2007**, *46* (23), 4293–4297.

(15) Alaerts, L.; Maes, M.; van der Veen, M. A.; Jacobs, P. A.; De Vos, D. E. *Phys. Chem. Chem. Phys.* **2009**, *11* (16), 2903–2911.

(16) Alaerts, L.; Maes, M.; Jacobs, P. A.; Denayer, J. F. M.; De Vos, D. E. *Phys. Chem. Chem. Phys.* **2008**, *10*, 2979–2985.

(17) Finsy, V.; De Bruyne, S.; Alaerts, L.; De Vos, D. E.; Jacobs, P. A.; Baron, G. V.; Denayer, J. E. M. *Stud. Surf. Sci. Catal.* **2007**, *170* (2), 2048–2053.

(18) Horcajada, P.; Serre, C.; Vallet-Regi, M.; Sebban, M.; Taulelle, F.; Ferey, G. *Angew. Chem., Int. Ed.* **2006**, *45* (36), 5974–5978.

(19) Serre, C. *Actual. Chim.* **2008**, (322), 15–19.

(20) Ferey, G. *Chem. Soc. Rev.* **2008**, *37*, 191–214.

(21) Rowsell, J. L. C.; Yaghi, O. M. *Microporous Mesoporous Mater.* **2004**, *73* (1−2), 3–14.

(22) Fletcher, A. J.; Thomas, K. M.; Rosseinsky, M. J. *J. Solid State Chem.* **2005**, *178* (8), 2491–2510.

(23) Kitagawa, S.; Uemura, K. *Chem. Soc. Rev.* **2005**, *34* (2), 109–119.

(24) Uemura, K.; Matsuda, R.; Kitagawa, S. *J. Solid State Chem.* **2005**, *178* (8), 2420–2429.

(25) Bureekaew, S.; Shimomura, S.; Kitagawa, S. *Sci. Technol. Adv. Mater.* **2008**, *9* (1), 1–12.

(26) Serre, C.; Millange, F.; Thouvenot, C.; Nogues, M.; Marsolier, G.; Louer, D.; Ferey, G. *J. Am. Chem. Soc.* **2002**, *124* (45), 13519–13526.

(27) Hamon, L.; Vimont, A.; Serre, C.; Devic, T.; Ghoufi, A.; Maurin, G.; Loiseau, T.; Millange, F.; Daturi, M.; Ferey, G.; De Weireld, G. In *Characterisation of Porous Solids*; Kaskel, S., Llewellyn, P., Rodriguez-Reinoso, F., Seaton, N. A., Eds.; RSC Publishing: Cambridge, U.K., 2009; pp 25−31.

(28) Coudert, F. X.; Jeffroy, M.; Fuchs, A. H.; Boutin, A.; Mellot-Draznieks, C. *J. Am. Chem. Soc.* **2008**, *130* (43), 14294–14302.

(29) Trung, T. K.; Trens, P.; Tanchoux, N.; Bourrelly, S.; Llewellyn, P.; Loera-Serna, S.; Serre, C.; Loiseau, T.; Fajula, F.; Ferey, G. *J. Am. Chem. Soc.* **2008**, *130* (50), 16926–16932.

(30) Llewellyn, P. L.; Maurin, G.; Devic, T.; Loera-Serna, S.; Rosenbach, N.; Serre, C.; Bourrelly, S.; Horcajada, P.; Filinchuk, Y.; Ferey, G. *J. Am. Chem. Soc.* **2008**, *130* (38), 12808–12814.

(31) Ghoufi, A.; Maurin, G. *J. Chem. Phys.* **2009**.

(32) Finsy, V.; Ma, L.; Alaerts, L.; De Vos, D. E.; Baron, G. V.; Denayer, J. F. M. *Microporous Mesoporous Mater.* **2009**, *120* (3), 221–227.

(33) Couck, S.; Denayer, J. E. M.; Baron, G. V.; Rémy, T.; Gascon, J.; Kapteijn, F. *J. Am. Chem. Soc.* **2009**, *131* (18), 6326–6327.

(34) Loiseau, T.; Serre, C.; Huguenard, C.; Fink, G.; Taulelle, F.; Henry, M.; Bataille, T.; Ferey, G. *Chem.—Eur. J.* **2004**, *10* (6), 1373–1382.

53(Cr) in PSA separations, by looking at both breakthrough and desorption curves.

Experimental Section

Synthesis. MIL-53(Cr) was synthesized on gram scale and activated in two steps according to the published procedures.[9,26] Further experiments were carried out directly on the powdered sample (particles size in the micrometer range) as-is after the synthesis and activation.

Gravimetry Measurements. The static coadsorption experiments were carried out according to the method described by Keller et al.[35,36] at 303 K up to 2.5 MPa using a laboratory made gas dosing system connected to a commercial gravimetric adsorption device (Rubotherm Präzisionsmesstechnik GmbH).[37−39] Prior to each experiment, the sample was outgassed at 523 K for 16 h. The gas mixtures were purchased preprepared (Air Liquide, Alphagaz). Three mixtures were studied with 25% mol., 50% mol. and 75% mol. CO_2 in CH_4. A step by step gas introduction mode was used and after each equilibrium point was reached, measurements of pressure, weight and gas density allow an estimation of the amount of each adsorbed component. For the calculations of mixture nonideality, the NIST Refprop data set was used.[40] A slight variation of the capacity at high pressure was observed between two different batches of synthesis (data in Figure 1, parts a and b were obtained with two different batches), but it did not affect the overall shape of the isotherms.

Adsorption Coupled with in Situ XRPD and Raman Spectroscopy. Combined in situ synchrotron X-ray powder diffraction (XRPD) and Raman spectroscopy experiments were carried out at the BM01A station at the Swiss Norwegian Beamline of the European Synchrotron Radiation Facility (Grenoble, France). The powdered sample was introduced in a 1 mm quartz capillary and connected to a homemade gas dosing system.[30,41] Prior to the experiments, the sample was outgassed under vacuum (pressure of about 10^{-3} mbar) at 473 K for a few hours. The temperature was then adjusted to 303 K, and doses of gas mixtures were introduced. XRPD were collected using a MAR345 imaging plate with a sample-to-detector distance of 400 mm ($\lambda = 0.699765$ Å). The data were integrated using the Fit2D program (Dr. A. Hammersley, ESRF) and a calibration measurement of a NIST LaB6 standard sample. The patterns were indexed using the Dicvol software.[42] Le Bail fits were then performed with Fullprof2k software package.[43,44] X-ray powder diffractograms were collected 1 min after the gas introduction, with an acquisition time of 30 s (rotation rate $1° \cdot s^{-1}$). New X-ray powder diffraction patterns were recorded at the same pressure every 5 min, and equilibrium (at a given pressure) was assumed when no change was observed between the successive patterns.

Raman spectra were collected in situ in the capillary at the position of the X-ray beam. The Renishaw confocal spectrometer was equipped with a laser at 532 nm and a 1800 lines·mm^{-1} grating. The laser and Raman signals were transferred between the spectrometer and the experimental hutch via optical fibers. Laser power on sample was $1-3$ mW, acquisition time varied from 1 to 15 min. Semiquantitative data were obtained from the integrated intensities of characteristic bands of the adsorbed gases, the ν_1 band at $\sim$1383 cm^{-1} for CO_2 and the ν_1 band at $\sim$2906 cm^{-1} for CH_4 and structural bands of the MIL-53 occurring in the same regions. The $2\nu_2$ and ν_1 bands at 1286 and 1388 cm^{-1} of CO_2 in the gas phase were shifted to lower wavenumbers at ca. 1281 cm^{-1} and 1383 cm^{-1} in the adsorbed state (see Figure S1), respectively. For CH_4, the ν_1 band was shifted from 2917 cm^{-1} in the gas phase to 2906 cm^{-1} in the adsorbed state. These red-shifts are attributed to the adsorption inside the *pores* of MIL-53(Cr) and lie in the range of those previously reported for the adsorption of CO_2 or CH_4 in zeolites,[45] in clathrates[46] or in IRMOF materials.[47] The shifts did not depend on the composition of the gas phase or on the pressure. In order to determine the NP/LP fractions, spectra were curve-fitted in the $1415-1475$ cm^{-1} region (see the Supporting Information for more details).

Breakthrough Curves Measurements. Breakthrough curve experiments were carried out with a column with a length of 8 cm and an internal diameter of 1.05 cm, packed with a powder sample. The column was placed into an oven and was outgassed at 473 K with a helium flow of 1 NL·h^{-1}. The same CO_2-CH_4 gas mixtures as for the gravimetric measurements were prepared via mass flow controllers (pure gases provided by Air Liquide). Breakthrough experiments were carried out by switching abruptly from He to CO_2-CH_4 mixtures (unless otherwise noted). The adsorbed amounts of CO_2 and CH_4 were calculated by mass balances. Breakthrough experiments were performed at pressures up to 1.0 MPa at 303 K with flow ranges from 0.5 to 4 NL·h^{-1} (see Supporting Information for more details). The pressure drop over the column was 1.7 at 10 bar, 0.7 at 5 bar and 0.35 at 1.0 bar. In the Figures, breakthrough curves are represented in the form of the normalized molar flow rates $F_i/F_{i,0}$, F_i being the measured flow rate of component i at the column outlet and $F_{i,0}$ being the feed flow rate of component i. The breakthrough experiments allowed us to calculate the selectivity of MIL-53(Cr) for CO_2, which is defined as $\alpha = (x_{CO2}/y_{CO2})/(x_{CH4}/y_{CH4})$, where x_i and y_i are the molar fractions of the compound i in the adsorbed and gas phases respectively.

Computational Details

Partial Charges and Interatomic Potential Parameters. The partial charges for all of the atoms of the framework were taken from our previous Density Functional Theory calculations.[48] The interatomic potential for the MIL-53(Cr) framework and the corresponding parameters are detailed in our previous article.[49] The CO_2 molecule was represented by a rigid point charge model with the following partial charges 0.6512 and -0.3256 (expressed in electron units) carried by the C and O atoms respectively, as reported by Harris and Yung.[50] The CH_4 molecule was also described by a rigid point charge model with the atoms carrying the partial charges (in electron units): C (-0.472) and H ($+0.118$).[51]

(35) Keller, J. U.; Staudt, R.; Tomalla, M. *Ber. Bunsen-Ges. Phys. Chem. Chem. Phys.* **1992**, *96* (1), 28–32.

(36) Keller, J. U.; Dreisbach, F.; Rave, H.; Staudt, R.; Tomalla, M. *Adsorpt.—J. Int. Adsorpt. Soc.* **1999**, *5* (3), 199–214.

(37) Dreisbach, F.; Seif, A. H. R.; Losch, H. W. *Chem. Ing. Tech.* **2002**, *74* (10), 1353–1366.

(38) De Weireld, G.; Frere, M.; Jadot, R. *Meas. Sci. Technol.* **1999**, *10* (2), 117–126.

(39) Ghoufi, A.; Gaberova, L.; Rouquerol, J.; Vincent, D.; Llewellyn, P. L.; Maurin, G. *Microporous Mesoporous Mater.* **2009**, *119* (1−3), 117–128.

(40) Kunz, O.; Klimeck, R.; Wagner, R.; Jaeschke, W., *The GERG-2004 Wide-Range Equation of State for Natural Gases and Other Mixtures*, Fortschr.-Ber. VDI, VDI-Verlag: Dusseldorf, Germany, 2007.

(41) Llewellyn, P. L.; Horcajada, P.; Maurin, G.; Devic, T.; Rosenbach, N.; Bourrelly, S.; Serre, C.; Vincent, D.; Loera-Serna, S.; Filinchuk, Y.; Ferey, G., submitted, 2009.

(42) Boultif, A.; Louer, D. *J. Appl. Crystallogr.* **1991**, *24*, 987–993.

(43) Rodriguez-Carvajal, J. In *Collected Abstracts of Powder Diffraction Meeting* **1990**, 127−128.

(44) Roisnel, T.; Rodriguez-Carvajal, J. In *Abstracts of the 7th European Powder Diffraction Conference*, Barcelona, Spain, 2000; p 71.

(45) de Lara, E. C. *Phys. Chem. Chem. Phys.* **1999**, *1* (4), 501–505.

(46) Sum, A. K.; Burruss, R. C.; Sloan, E. D. *J. Phys. Chem. B* **1997**, *101* (38), 7371–7377.

(47) Siberio-Perez, D. Y.; Wong-Foy, A. G.; Yaghi, O. M.; Matzger, A. J. *Chem. Mater.* **2007**, *19* (15), 3681–3685.

(48) Ramsahye, N. A.; Maurin, G.; Bourrelly, S.; Llewellyn, P.; Loiseau, T.; Ferey, G. *Phys. Chem. Chem. Phys.* **2007**, *9* (9), 1059–1063.

(49) Salles, F.; Ghoufi, A.; Maurin, G.; Bell, R. G.; Mellot-Draznieks, C.; Ferey, G. *Angew. Chem., Int. Ed.* **2008**, *47* (44), 8487–8491.

(50) Harris, J. G.; Yung, K. H. *J. Phys. Chem.* **1995**, *99* (31), 12021–12024.

(51) Rosenbach, N.; Jobic, H.; Ghoufi, A.; Salles, F.; Maurin, G.; Bourrelly, S.; Llewellyn, P. L.; Devic, T.; Serre, C.; Ferey, G. *Angew. Chem., Int. Ed.* **2008**, *47* (35), 6611–6615.
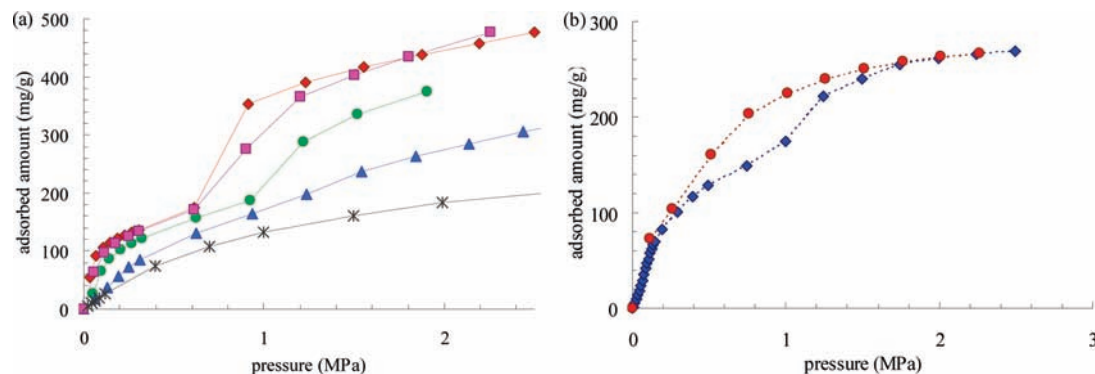
Figure 1. (a): Total adsorbed amount at 303 K on the MIL-53(Cr) (◇: pure CO_2; □: gas mixture 75–25 CO_2–CH_4; ○: gas mixture 50–50 CO_2–CH_4; △: gas mixture 25–75 CO_2–CH_4; *: pure CH_4). (b): Adsorption (blue diamonds) and desorption branch (red circles) of the 75–25 CO_2–CH_4 mixture isotherm.

All the crossed Lennard–Jones (LJ) parameters were calculated using the Lorentz–Berthelot combining rules.

Adsorption Isotherms. The absolute adsorption isotherms for CO_2 and the 3 different gas mixtures were first computed for both rigid NP and LP forms at 303 K up to 3 MPa using Grand Canonical Monte Carlo (GCMC) simulations.[52] The crystallographic coordinates of both NP and LP were taken from the previous XRPD investigations.[9,26] These calculations were performed using a simulation box corresponding to 32 unit cells with 5×10^7 MC steps. The LJ interactions were evaluated using a spherical cutoff of 12 Å, while the electrostatic interactions were computed using the Ewald summation[53] with a precision of 10^{-5}. The chemical potentials of the pure components and the 3 different mixtures were calculated using the classical test particle Widom insertion method from the NPT statistical ensemble.[53] This approach has been described in detail elsewhere.[39] A further step consisted of building the composite isotherm for CO_2 and 3 phase mixtures from the calculated adsorption isotherms in the rigid LP and NP structures and from the fractions of both forms estimated by Raman Spectroscopy. Regarding CH_4, the calculations were performed only in the LP form since previous in situ XRPD studies clearly showed that the MIL-53(Cr) system does not undergo any significant modification of the unit cell parameters up to high pressure.[51] The selectivities at low pressure were calculated using the same equation as mentioned above.

Additional calculations were performed using a Hybrid Monte Carlo (HMC) approach in the osmotic statistical ensemble to be able to follow the evolution of the composition of the adsorbed gas mixture when the MIL-53(Cr) switches from the LP to the NP form. This method has already been successfully applied for dealing with the adsorption of CO_2 in MIL-53(Cr) where the framework was treated as fully flexible by means of our own force field.[31] As a typical illustration, one calculation was performed at 300 K for the gas mixture (50–50) imposing a pressure of 0.2 MPa. All of the details of the HMC procedure can be found in our previous work.[31]

Results

Gravimetry Experiments. Figure 1 compares previous gravimetric measurements for pure CO_2 and CH_4[5] with coadsorption measurements of 25–75, 50–50, and 75–25 CO_2–CH_4 mixtures (molar ratios).

The isotherms of the pure CO_2 component and those of the gas mixtures exhibit a clear step at intermediate pressure. The

step becomes less pronounced as the CH_4 content of the mixture increases and totally disappears for pure CH_4.[54,55]

For the binary mixtures, the total mass uptake shown in Figure 1 was decomposed into the contribution of CO_2 and CH_4. The concentration of CO_2 and CH_4 in the gas phase was deduced from the measurement of gas phase density via an equation of state and the composition of the adsorbed phase was then calculated from the mass balance.[35,36] The results are shown in Figure 2. The uncertainties of adsorbed quantities are estimated to be less than ±0.5 mmol/g for CO_2 and ±1.0 mmol/g for CH_4. Figure 2 also contains the coadsorption isotherms obtained from Raman spectroscopy and from molecular simulation; these will be discussed later in the text.

Figure 2, parts (b)–(d), shows that the adsorbed phase is always richer in CO_2 than in CH_4. For the 25–75 CO_2–CH_4 gas mixture, the CO_2 adsorption isotherm is of type I and the adsorbed amount of CH_4 increases almost linearly with pressure. For the equimolar mixture, a step is observed in the CO_2 adsorption isotherm at around 1.0 MPa. The steps shifts to 0.6 MPa for the 25–75 mixture. The adsorbed amount of CH_4 remains very small in both cases. In analogy to pure CO_2, the step in the mixture isotherms (observed when the gas phase concentration of CO_2 is at least 50%) is most likely due to the transformation of the NP to the LP form. Combined in situ XRD and Raman spectroscopy measurements of MIL-53(Cr) were thus performed to gain more detailed insight in the breathing behavior.

In Situ XRPD and Raman Spectroscopy. In situ XRPD patterns of MIL-53(Cr) during the adsorption of the three different mixtures of CO_2 and CH_4 were collected up to 1.5–3.0 MPa at 303 K. The resulting XRPD patterns strongly depend on the composition (Figure 3). For a mixture poor in CO_2 (CO_2–CH_4 ratio of 25–75), only the LP form is present over the whole range of pressures, with a very slight increase of the unit cell volume at higher pressures (1.4% at 30 bar, see Table S1 in Supporting Information). Alternatively, for the CO_2 rich mixtures (CO_2–CH_4 ratio of 50–50 and 75–25), mixtures of NP and LP forms appear at intermediate pressures, while only the LP form is present at low and high pressures. The cell volume of the LP form slightly increases with pressure (1.3 and 1.5% at 25 and 27 bar for the 50–50 and 75–25 mixtures, respectively) as already observed with pure CO_2.[5] On the whole,

(52) Gupta, A.; Chempath, S.; Sanborn, M. J.; Clark, L. A.; Snurr, R. Q. *Mol. Simul.* **2003**, *29* (1), 29–46.
(53) Frenkel, D.; Berend, S. *Understanding Molecular Simulations: From Algorithm to Applications*; Academic Press: New York, 2002.

(54) Sing, K. S. W. *Pure Appl. Chem.* **1985**, *57* (4), 603–619.
(55) Rouquerol, F.; Rouquerol, J.; Sing, K. S. W. *Adsorption by Powders and Porous Solids*, Academic Press: London, San Diego, 1999.
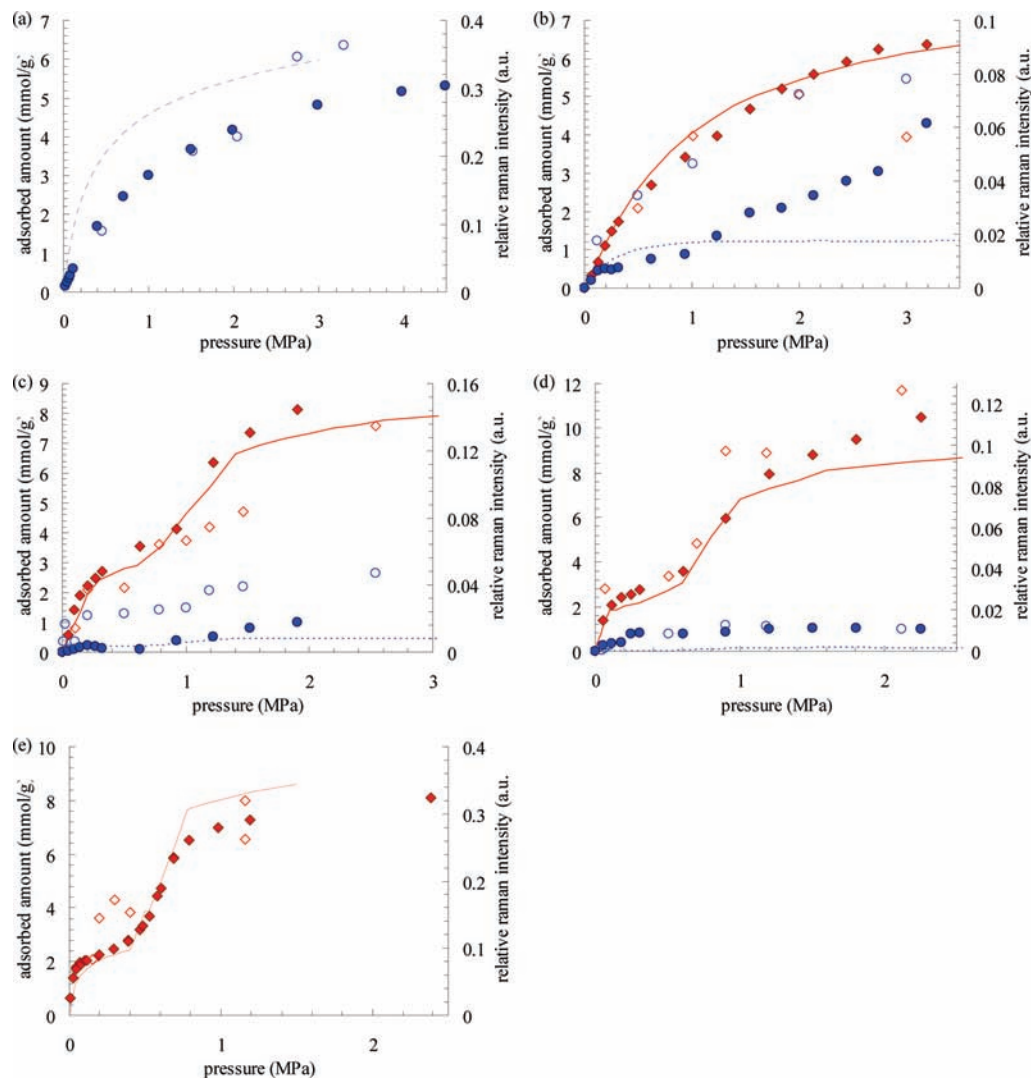
Figure 2. CO_2 (◆) and CH_4 (●) adsorption isotherms at 303 K on the MIL-53(Cr) compared to the relative Raman intensity of CO_2 (◇) and CH_4 (○), and the simulations (CO_2: full line; CH_4: dashed line).[52] Gas compositions CO_2–CH_4: 0−100 (a), 25−75 (b), 50−50 (c), 75−25 (d), and 100−0 (e); red: CO_2; blue CH_4.

the behavior of MIL-53(Cr) upon adsorption of CO_2–CH_4 mixtures closely follows the pure components CO_2 and CH_4: no structural modification (LP form only) takes place for the CH_4-rich mixture, while the solid "breathes" upon adsorption of CO_2-rich mixtures, with two consecutive structural switches from LP to NP at low pressure and from NP to LP at higher pressure. Compared to pure CO_2, the NP to LP transition is attenuated and mixtures of NP and LP forms coexist at lower and intermediate pressures, probably in the form of separate crystalline domains (particles). On the basis of the maximum of intensity for the NP form, the NP/LP ratio increases with the amount of CO_2 in the gas mixture. Unfortunately, no quantification is feasible, as the intensity of the diffraction peaks is dependent on the pore content, which significantly changes with the pressure.

The unit cell volumes of both the LP (see above) and NP forms remain almost constant, and independent of the mixture. The volume of the NP form depends on the size of the occluded guest.[30] Here, its cell volume lies in the 1082−1095 Å³ range, very similar to the one of pure CO_2 at the same temperature (1088 Å³).(Unit-cell of the *narrow pore* form upon adsorption of CO_2 ($p = 0.2$ MPa) at 303 K: monoclinic *C2/c*, $a = 19.692(2)$ Å, $b = 8.4547(7)$ Å, $c = 6.8054(6)$ Å, $\beta = 106.210(9)°$, $V =$

1088.0(2) Å³.) This suggests that, although the composition of the CO_2–CH_4 mixture changes, the gas adsorbed in the NP form contains solely (or mainly) CO_2 molecules.

The Raman spectra, measured simultaneously with the XRPD patterns, were used to provide an estimation of the composition of the adsorbed phase as well as of the LP/NP ratio. This unusual determination of the extent of breathing correlates well with the qualitative data obtained by XRPD. For evaluating the LP/NP ratio, the relative intensities of the characteristic bands at ~1432 and 1444 cm⁻¹ were used (ν_{sym}(COO) vibration).[56] The band at 1432 cm⁻¹ is characteristic for the NP form, while the band at 1444 cm⁻¹ carries the signature of the LP form (Figure S3 of the Supporting Information). The results of the deconvolution of the Raman spectra are represented in Figure 4. Figure 4 shows that, for the CO_2-rich mixture, the fraction of the NP form is at its maximum between 0.15 and 0.5 MPa. In the case of the 50−50 and 25−75 mixtures, the maximum is found at a higher pressure and the conversion from LP to NP decreases with increasing CH_4 content. The partial pressure of CO_2 at which the fraction of the NP form reaches its maximum is

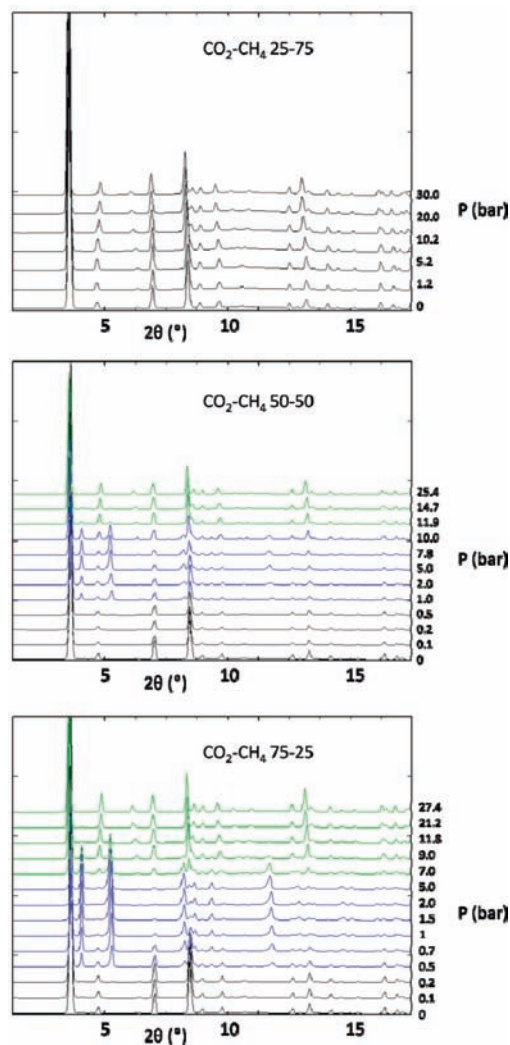(56) Arenas, J. F.; Marcos, J. I. *Spectrochim. Acta, Part A* **1979**, *35* (4), 355–363.

Figure 3. Adsorption of mixtures of CO₂ and CH₄ on MIL-53(Cr) at 303 K followed by in situ XRPD (left). The color on XRD plots corresponds to the major phase observed at the given pressure; black: *large pore* form (low pressure); blue: *narrow pore* form; green: *large pore* form (high pressure).
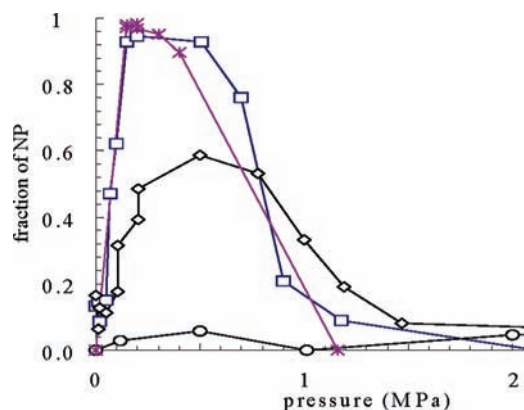

Figure 4. Fraction of the NP form as calculated from Raman results for gas feed CO₂−CH₄: 100−0 (*), 75−25 (□), 50−50 (◇), and 25−75 (○).

similar for both mixtures and is only slightly higher than the value for pure CO₂. This indicates that the partial pressure of CO₂ controls the closing of the structure while the presence of CH₄ decreases the extent of the LP to NP conversion. This
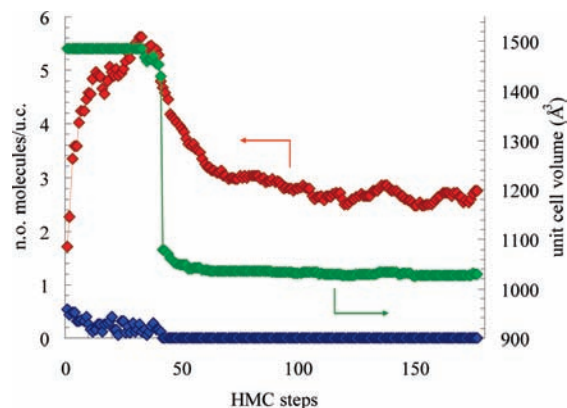

Figure 5. Adsorbed amounts of CO₂ (red) and CH₄ (blue) and unit cell volumes of MIL-53(Cr) (green) as a function of the HMC steps, simulated for a 50−50 gas mixture at 303 K and 0.2 MPa.

observation strengthens the hypothesis of the absence of methane adsorbed within the pores of the NP form (since CH₄ prefers to be in the LP form its coadsorption in the NP form is expected to narrow down the CO₂-partial pressure range where the NP form is stable).

Further, integration of the Raman band intensities of adsorbed CH₄ and CO₂ allowed us to extract the adsorption isotherms and compare them to those obtained from gravimetry (Figure 2). In case of pure CO₂ and CH₄ the evolutions of the Raman data are in good agreement with the gravimetry. However, for the CO₂−CH₄ mixtures, Raman tends to overestimate the adsorbed amount of methane compared to the gravimetry measurements. Nevertheless, these results show that Raman spectroscopy is a useful tool to follow the concentrations of the adsorbed phase in situ, and that it might be used to follow an adsorption column operando.

Simulations. Figure 2, parts a and e, compares the simulated absolute isotherms for pure CH₄ and CO₂ on the MIL-53(Cr) at 303 K to those from gravimetry. The calculations reproduce fairly well the experimental data for the pure components, which validates our approach. As previously pointed out, the CO₂ mainly interacts with the μ_2−OH groups at the surface of the NP and LP forms, while the CH₄ is homogeneously distributed within the pore of the LP form. The isotherms of the gas mixtures were constructed as composite isotherms, by combining simulations in the LP and NP form, the fraction LP/NP being taken from Raman spectroscopy (Figures 2, parts b−d). This "composite" approach leads to a good agreement with the gravimetric measurements for both 50−50 and the CO₂-rich 75−25 mixtures while predictions overestimate the adsorbed amount of CH₄ for the CH₄-rich 25−75 mixture. Further, the simulations show that the NP form, with a cell volume of 1088 Å³ can only accommodate CO₂ molecules. This clearly emphasizes that under thermodynamic equilibrium, the CH₄ molecules cannot be included in the NP structure. In the composite approach, crystallites in the LP form containing both CH₄ and CO₂ molecules coexist with crystallites in the NP structure with only CO₂ molecules inside the pore. The arrangements of both CO₂ and CH₄ in LP form do not differ from those observed for the single component adsorption.

A further evidence of the absence of CH₄ in the NP form was obtained via Hybrid Monte Carlo (HMC) simulations performed on the phase mixture (50−50) starting with the LP form and imposing a pressure of 2 bar at 303 K (Figure 5). The structural transition from the LP to the NP form which occurs
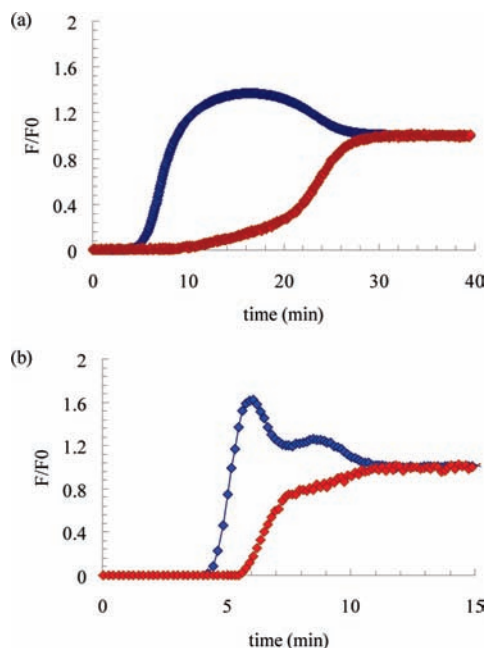
Figure 6. Breakthrough curve of binary CO_2–CH_4 mixtures on MIL-53(Cr) at 303 K: CO_2 in red, CH_4 in blue. Gas feed CO_2–CH_4: (a) 50–50 at 0.1 MPa and (b) 75–25 at 1.0 MPa.

after 40 HMC steps, is clearly accompanied by a complete desorption of the CH_4 molecules. While the simulated number of CH_4 molecules is zero in the NP form, the amount of CO_2 fluctuates around 3 molecules per unit cell in very good agreement with the experimental data (see Figure 2e). Further, the selectivities of CO_2 over CH_4 calculated in the LP form at low pressure are similar for the three different gas mixtures and centered around 5.

Breakthrough Experiments. Breakthrough experiments were carried out to evaluate the separation performance of MIL-53(Cr). Via mass balances they allow us to calculate the adsorbed quantities and the selectivities in the coadsorption of CO_2 and CH_4. Moreover, they contain information about the adsorption dynamics and could carry the signature of LP–NP transitions if they occur during the breakthrough curve. In order to check the coherence of gravimetry measurements and breakthrough curves, pure CO_2 and CH_4 adsorption isotherms have first been measured by both methods (see Supporting Information). These results are in excellent agreement (error <5%).

Figure 6a shows the breakthrough curve of a 50–50 CO_2–CH_4 mixture at 0.1 MPa. As expected, CH_4 is the least adsorbed component. It breaks first and its breakthrough curve presents a small "roll-up", i.e., the flow rate temporarily exceeds the feed flow rate. The roll-up can be attributed to the desorption of CH_4 induced by CO_2, when the concentration front of CO_2 advances through the column. The slope of the CO_2 break-through curve (Figure 6a) is initially rather small, which indicates that the substitution of CH_4 by CO_2 in the adsorbed phase is slow. After 20 min, the slope clearly increases. The change of the slope is most likely related to the breathing of the structure.

For the 75–25 mixture at 1.0 MPa (Figure 6b), an opposite change in slope is observed. The CO_2 breakthrough is initially steep and then flattens out. The breakthrough curve of CH_4 exhibits two peaks. The appearance of the second peak coincides with the change of the slope of the CO_2 concentration front.

The same phenomenon is observed in the breakthrough curve of this mixture at 0.5 MPa (see Supporting Information). Similar breakthrough curves with a double roll-up of CH_4 have already been observed by Finsy et al. on MIL-53(Al)[32] and by Couck et al. on the amino functionalized MIL-53(Al).[33]

Analysis of the Desorption and of the Hysteresis. For practical applications in PSA process, the desorption behavior is of a high interest. The desorption of pure CO_2[8] follows a hysteresis loop. The structure closes at a much lower pressure than it opens during the adsorption. A hysteresis is also observed during the desorption of 25–75 and 75–25 CO_2–CH_4 gas mixtures (Figure 1 and Figure S4 of the Supporting Information). Hysteresis is usually the signature of metastability. In the region of intermediate pressures, the system does not reach the same state, depending on whether we start from the NP form (in the adsorption branch) or from the LP form (in the desorption branch). To investigate the effect of this metastability on the breakthrough curves, two sets of experiments were performed on a column initially saturated with CO_2. First, a 25–75 CO_2–CH_4 mixture was injected into the column that had been presaturated either with a 25–75 CO_2–He mixture or with pure CO_2 at 1.0 MPa. In the former case, MIL-53(Cr) was initially in the NP form filled with CO_2, in the latter case the solid was in the LP-form (filled with CO_2) at the beginning of the experiment (Table 1). Figure 7a compares the CH_4 breakthrough curves obtained on the columns presaturated with CO_2 with the one measured on an initially empty column. The difference is striking. When MIL-53(Cr) is in the NP form filled with CO_2, CH_4 breaks immediately and the adsorbed amount of CH_4 is close to zero, in agreement with previous results obtained with the NP hydrated MIL-53(Cr) solid.[8] Further, when MIL-53(Cr) is presaturated with CO_2 in the LP form, CH_4 also breaks immediately, which indicates that its adsorption is slow, but in fine the adsorbed amount of CH_4 is close to the one found when starting from an empty column. A second set of experiments was performed with a 75–25 CO_2–CH_4 mixture with a column either presaturated using a 75–25 CO_2–He mixture (LP + NP forms) or with pure CO_2 (LP form only). Again, CH_4 break-through curves were measured in the two cases and compared with the one for CH_4 measured on an initially empty column (Figure 7b, Table 1). Starting from the partially closed MIL-53(Cr) solid, the adsorbed amount of CH_4 is low but different from zero. When one starts from the fully open form filled with CO_2, the adsorbed amount of CH_4 is higher than that when the column is initially empty, presumably because we move on the desorption branch of the hysteresis and therefore end up with a higher fraction of the LP form at the end of the experiment.

Discussion

Effect of Coadsorption of CO_2 and CH_4 on the Breathing of MIL-53(Cr). Under vacuum at room temperature, the MIL-53(Cr) solid is in its LP form, which is thermodynamically more stable. Adsorption of CO_2 induces the transformation of the LP to the NP form. This transformation occurs at low pressure (20 kPa). At 0.4 MPa, the structure starts to switch back to the LP form which has a larger pore volume and hosts larger amounts of CO_2. In coadsorption with CH_4, the total pressure required to close the structure increases (Figure 3) while for a low CO_2 concentration in the mixture, i.e., 25%, the MIL-53(Cr) does not close anymore. These trends are qualitatively in line with very recent theoretical calculations.[57] Interestingly, the partial pressure of CO_2, which corresponds to the maximum of the fraction of the NP form is similar for the 50–50 and the 75–25

Table 1. CH₄ Adsorbed Quantities (mmol·g⁻¹) at 1.0 MPa for 25−75 and 75−25 CO₂−CH₄ Gas Mixtures for Different Initial Saturations of the Column

	25−75			75−25		
CO₂−CH₄ mole fraction in feed	CH₄ adsorbed amount (mmol·g⁻¹)	initial state	final state	CH₄ adsorbed amount (mmol·g⁻¹)	initial state	final state
saturation by pure CO₂	2.89	LP−CO₂	LP	1.37	LP−CO₂	LP
saturation by CO₂−He	0.00	NP−CO₂	NP	0.33	LP−CO₂	**LP** + NP
without initial saturation	2.92	LP−empty	LP	0.99	LP empty	**LP** + NP

CO_2−CH_4 mixtures and is not far from the value obtained for the pure CO_2. This indicates that the driving force for the LP to NP transformation is the partial pressure of CO_2. CH_4 does not contribute to the closing of the structure, but a high concentration of CH_4 in the mixture totally or partially inhibits the LP to NP transition.

The same holds true for the NP to LP transition at higher pressure. The absolute pressure at which this transition starts, increases with the concentration of CH_4 in the mixture, but the partial pressure of CO_2 which induces the opening of the structure, remains more or less constant.

Effect of Flexibility on the Breakthrough Curves. The breakthrough curves of the mixtures exhibit interesting phenomena related to the flexibility of the structure. Gravimetry, in situ XRPD and Raman spectroscopy show that when the composition of the gas mixture is constant as the pressure of the gas mixture increases, consecutive transitions from LP to NP and from NP to LP occur. In breakthrough experiments, however, the pressure is constant and the composition of the gas mixture at the column exit evolves with time. Starting with pure CH_4 at the beginning of the breakthrough, the CH_4 content gradually decreases until the gas mixture finally reaches the feed composition. From the Raman results, we can derive (Figure S9 of the Supporting Information) how the NP/LP fraction evolves when one moves at constant pressure from pure CH_4

to pure CO_2. At low pressures, the NP fraction increases with the molar fraction of CO_2, while at 1.0 MPa, it runs through a maximum, and at 2.0 MPa, the structure is open, which is in qualitative agreement with recent theoretical predictions.[57] These results will guide our interpretation of the breakthrough curves.

During adsorption of a 25−75 CO_2−CH_4 mixture, MIL-53(Cr) always remains in the LP configuration, like with pure CH_4. The resulting breakthrough curves showing a conventional behavior (see Figures S5a, S6a, S7a of the Supporting Information). For the 50−50 CO_2−CH_4 mixtures, a partial transformation of LP to NP takes place. The downstream end of the column is first in contact with pure CH_4, and then the concentration of CO_2 gradually increases up to the final 50−50 composition. When moving from pure CH_4 to a 50−50 mixture at 0.1 MPa, the structure initially in its LP form partially closes, as the concentration of CO_2 increases (Figure S8 of the Supporting Information). The slope of the CO_2 breakthrough curve is initially low (Figure 6a). The pores of MIL-53(Cr) are open and the thermodynamic driving force for replacing CH_4 by CO_2 is small, due to the relatively weak CO_2 interaction within the LP form.[58,59] This leads to a dispersed front with a low slope. Once the mixture reaches the required CO_2 concentration, CO_2 succeeds in closing the pores and as the affinity for CO_2 drastically increases (enthalpies of adsorption of CO_2 in the LP and the NP forms are about 24 kJ·mol⁻¹ and 35 kJ·mol⁻¹, respectively)[9] a change of the slope of the breakthrough curve occurs.

In the case of the 75−25 CO_2−CH_4 mixture at 1.0 MPa (Figure 6b), the MIL-53(Cr) structure is initially open and gradually closes as the CO_2 concentration increases. At the end of the breakthrough curve, the CO_2 concentration is so high that the pores reopen in order to accommodate more CO_2 molecules. This releases some CH_4 molecules, which had apparently been trapped in the NP form, and leads to the second peak (the double roll-up) in the CH_4 breakthrough curve. Moreover, the transformation from NP to LP reduces the affinity toward CO_2 and thereby triggers the change in the slope of the CO_2 breakthrough curve.

We have also considered two alternative explanations for the double roll-up of CH_4. Couck et al.[33] observed a similar second peak in the CH_4 breakthrough curve, but no simultaneous change in the slope of the CO_2 breakthrough, and attributed the phenomenon to the expulsion of CH_4 from the structure when it **closes**. Expulsion of CH_4 from MIL-53(Cr) upon closing of the structure is indeed deduced from our molecular simulations. Yet, assigning the double roll-up of CH_4 to an LP to NP transformation does not explain the
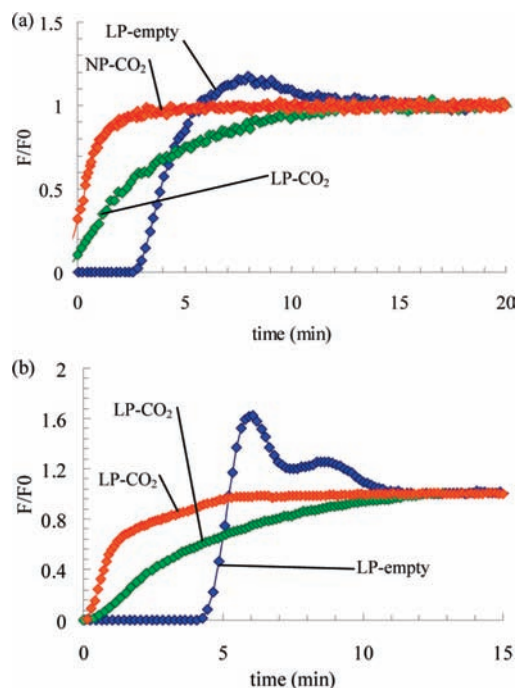

Figure 7. CH₄ breakthrough curves at 303 K and 1.0 MPa for two CO₂−CH₄ gas mixture ratios: (a) 25−75 or (b) 75−25. After initial saturation of the column with pure CO₂ (green), after initial saturation with 25−75 (a) or 75−25 (b) CO₂−He gas mixture (orange), and without initial saturation (blue).

(57) Coudert, F. X.; Mellot-Draznieks, C.; Fuchs, A. H.; Boutin, A. *J. Am. Chem. Soc.* **2009**, *131* (32), 11329–11331.
(58) Ramsahye, N. A.; Maurin, G.; Bourrelly, S.; Llewellyn, P. L.; Loiseau, T.; Serre, C.; Ferey, G. *Chem. Commun.* **2007**, (31), 3261–3263.
(59) Ramsahye, N. A.; Maurin, G.; Bourrelly, S.; Llewellyn, P. L.; Devic, T.; Serre, C.; Loiseau, T.; Ferey, G. *Adsorpt.−J. Int. Adsorpt. Soc.* **2007**, *13* (5−6), 461–467.
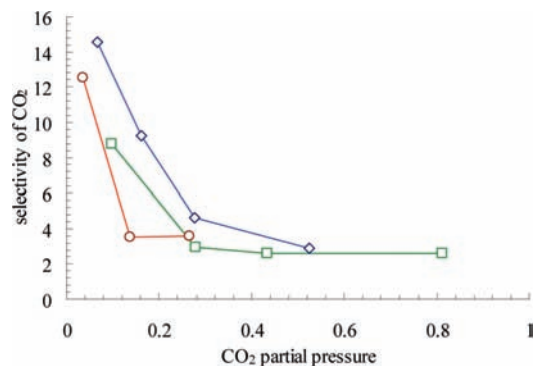
Figure 8. Selectivity of MIL-53(Cr) for CO_2. Breakthrough measurements, gas feed CO_2–CH_4: 75–25 (□), 50–50 (◇), and 25–75 (○).

simultaneous change in slope observed in the breakthrough curve of CO_2. We therefore attribute the second CH_4 peak to the **opening** of the structure. A second tentative explanation for the double roll-up of CH_4 would be thermal effects (the arrival of a temperature front at the column exit), linked to the strong exothermic character of the CO_2 adsorption. This option cannot be entirely ruled out.

Selectivity of MIL-53. To design a separation processes (PSA) using MIL-53(Cr) as a separating agent, the CO_2–CH_4 selectivity is an important criterion. The two crystallographic LP and NP structures can be considered as two different adsorbent materials, with different enthalpies of adsorption and different Henry constants and therefore different CO_2–CH_4 selectivities. Our results suggest that the NP form has a stronger affinity for CO_2 and virtually excludes CH_4, as already reported by Couck et al. for the amino-modified MIL-53(Al).[33] This is validated by molecular simulation, which clearly highlights the complete desorption of CH_4 as soon as the LP form switches to the NP version (Figure 5). Further, the various experimental data evidence that: (i) the cell volume of the NP form is constant and corresponds to the one found in presence of pure CO_2; (ii) the opening and closing of the structure are only controlled by the partial pressure of CO_2; (iii) if one starts breakthrough curves from the NP form filled with CO_2, the adsorption of CH_4 is indeed zero (this result was also confirmed by in situ Raman spectroscopy).

When NP and LP forms coexist in contact with CO_2–CH_4 mixtures, the NP form contains mainly CO_2, while the LP form coadsorbs both CO_2 and CH_4 with much lower selectivity. The overall selectivity measured experimentally should be correlated to the LP/NP fraction, i.e., one expects a high overall selectivity when the NP form is predominant and a low overall selectivity when the sample mainly contains the LP version. This result is indeed found in the molecular simulations.

The selectivities determined from breakthrough curves show qualitatively the same trend (Figure 8). The CH_4-rich mixture has the lowest CO_2/CH_4 selectivity, but the difference between CH_4-rich and CO_2-rich mixtures is strongly attenuated. The reason may be 2-fold. First, it is possible that thermodynamic equilibrium is not reached during the breakthrough experiments. The contact time is rather short and if the LP-NP transition has a significant kinetic barrier, it may not occur to the same extent as in the static XRPD and Raman experiments with long equilibration times. There is also some experimental evidence that CH_4 might be trapped in the NP form during the breakthrough experiments (see Figure 6a). All of these factors taken together could explain why the expected large difference

in selectivity between LP and NP forms is not observed in the breakthrough experiments after all.

Compared to the selectivity values measured with the same technique by Finsy et al. on MIL-53(Al),[32] our selectivities are lower, but the trend is the same, with a decreasing selectivity when the pressure increases.

Metastability and Hysteresis. The adsorption–desorption isotherms of pure CO_2 and of CO_2–CH_4 binary mixtures are characterized by the presence of hysteresis. Previous measurements with pure CO_2 showed that during the desorption, MIL-53(Cr) remained in the LP form from the plateau at high pressure down to the plateau at 0.2 MPa and then closed, the rest of the desorption branch being superposed with the adsorption branch.[9] The presence of this hysteresis loop suggests a metastable state. Further, application of the phase law to the two forms of MIL-53 indicates that the LP and NP forms can only be in equilibrium at a precisely given pressure (for a given gas phase composition). The fact that we observe a coexistence of the two phases over large range of pressures, in particular in the cases of the 75–25 and 50–50 CO_2–CH_4 mixtures, must therefore be the consequence of metastability (although we cannot totally exclude that the pressure of the LP-NP transition may depend on crystallite size, defect density, etc., which may also spread the transition over a small pressure range). As a consequence, the coadsorption results depend on the initial state of the system and on the manner that the experiment is performed. Indeed, breakthrough experiments performed with different initial saturations of the column by CO_2 prove that the initial state of the MIL-53(Cr) influences the final state (Table 1). If the solid is in the NP form filled with CO_2 before CH_4 is introduced, then the adsorbed amount of CH_4 is close to zero. But when initially saturated with pure CO_2 in the LP form before a CO_2/CH_4 is introduced, the amount of CH_4 adsorbed may even be higher than when starting from an empty MIL-53(Cr) because we move on the desorption branch of the hysteresis.

Conclusions

The coadsorption of CO_2 and CH_4 in the flexible MIL-53(Cr) structure using a large variety of techniques has shed light onto its complex behavior. CO_2-rich and equimolar CO_2–CH_4 mixtures lead to a breathing of the MIL-53(Cr) structure, i.e., an LP to NP transition and then back to LP form as the pressure increases. CH_4-rich mixtures ($\geq$75% CH_4) always maintain the solid in the LP form as with pure CH_4. The closing and opening of the structure is entirely controlled by the partial pressure of CO_2. CH_4 only has an influence on the extent of the transition. The structure can fully close when the CH_4 content is low (25%), for equimolar mixtures the closing remains partial.

Experimental results suggest that CH_4 is probably not adsorbed at all in the NP-form when it is filled with CO_2 (likewise, CH_4 does not adsorb in the NP form filled with H_2O),[8] in accordance with molecular simulations, which show that CH_4 is expelled from the structure when the LP to NP transition occurs. The exclusion of CH_4 from the NP structure lets us expect a very high CO_2–CH_4 selectivity in breakthrough experiments, carried out under conditions in which the NP form should dominate. However, experimentally measured selectivities were much lower, probably due to a kinetic barrier for the LP to NP transition which is not completed during the breakthrough experiments.

Structural metastability, probably also dependent on the heterogeneity of the sample, is an inherent feature of MIL-53(Cr) upon coadsorption of CO_2 and CH_4. The phase rule predicts that the NP and LP form of MIL-53(Cr) can only coexist at one given pressure and composition. In practice, however, coexistence of the two phases is observed over a large range of conditions, which makes the system difficult to predict because the final coadsorption state depends on the starting point of the system, especially in breakthrough experiments where the contact time with the gas mixture is low.

Concerning the use of MIL-53(Cr) in a PSA system, the step of the CO_2 adsorption isotherm at intermediate pressures looks very promising because it could potentially translate into a high working capacity between, for example, 0.2 and 1.0 MPa. Yet, other features make the system less attractive: the selectivity for CO_2 at high pressure is rather low and the large hysteresis means that the regeneration (the desorption) of the column occurs at a lower pressure than desirable. The ideal solid would be flexible at intermediate pressure, but have a narrow hysteresis loop to facilitate desorption. This would be possible by decreasing the LP−NP barrier, which paves the way for the line of future research.

Supporting Information Available: Breakthrough curve apparatus, CO_2−CH_4 breakthrough curves, Raman spectroscopy fraction of NP/LP, and full adsorption−desorption isotherms. This material is available free of charge via the Internet at http://pubs.acs.org.

JA907556Q